# Lubrication of the tire/road interface by fine particles: Tribological approach

**Y. Hichri[1], V. Cerezo[2], MT. Do[3] et H. Zahouani[4]**

[1] IFSTTAR, AME, EASE, yosra.hichri@ifsttar.fr
[2] IFSTTAR, AME, EASE, veronique.cerezo@ifsttar.fr
[3] IFSTTAR, AME, EASE, minh-tan.do@ifsttar.fr
[4] Laboratory of Tribology and Dynamic of Systems, University of Lyon, ENISE- ECL-ENTPE. UMRS CNRS 5513, hassan.zahouani@enise.fr

## Résumé :

*Le risque d'accidents augmente quand il pleut après une longue période sèche. Ce phénomène s'explique par la présence de particules fines qui s'accumulent sur la surface de chaussée pendant les périodes sèches et provoque une perte d'adhérence entre le pneu et la chaussée. Dans cet article, nous étudions l'action des particules routières pendant la période sèche en utilisant deux approches développées dans le domaine de la tribologie : l'approche du troisième corps, en particulier l'analyse de masses, pour comprendre le mouvement des particules à l'interface pneu/chaussée ; et les théories de lubrification sèche développées pour les poudres (comme le disulfure de molybdène MoS2) pour comprendre et modéliser le frottement. Des expérimentations sont menées en laboratoire afin de comprendre et modéliser cette action. Le protocole d'essai permet de simuler le processus de dépôt des particules sur la surface de chaussée. La surface des échantillons, représentative d'une surface de chaussée comporte une échelle de microtexture, représentant les aspérités des granulats, et une échelle de macrotexture, représentant l'espace entre les granulats. Les mesures de frottement sont réalisées avec le Pendule SRT, appareil couramment utilisé dans le domaine routier, qui simule le frottement par glissement d'un patin de gomme à 3 m/s sur la surface testée. Sur une surface initialement recouverte par des particules, des mesures successives de frottement sont réalisées, sans réapprovisionnement de particules entre deux mesures consécutives. Les échantillons sont pesés avant et après chaque mesure de frottement. Les résultats montrent que le coefficient de frottement chute significativement quand la surface est recouverte de particules en comparaison de celui mesuré sur une surface propre. Les passages successifs du patin de mesure induisent une remontée du coefficient de frottement jusqu'à atteindre une valeur stable qui reste inférieure à celle d'une surface propre. Trois flux de particules sont calculés : particules éjectées de l'aire de contact patin de frottement/surface d'échantillon ; particules piégées dans la microtexture ; et particules stockées dans la macrotexture. Une corrélation étroite est trouvée entre le coefficient de frottement et le flux de particules piégées dans la microtexture. Des similitudes ont été trouvées, en termes de mécanismes de lubrification, entre le comportement des particules étudiées et celui des poudres. Une première tentative de modélisation permet de calculer le coefficient de frottement à partir de la fraction de surface recouverte de particules.*

**Mots clefs :** *Frottement, revêtement de chaussée, particules fines, lubrification, modélisation*

# Abstract :

*Accidents increase during the first rain after a long dry period. This trend is due to the accumulation of fine particles originated from different sources such as atmosphere, road and tires debris, fuel emissions, etc. These particles accumulate on the road surface during a long dry period and induce a friction loss between the tire and the road surface. In this paper, we investigate the action of the particles during a dry period using two approaches developed in tribology: the third body approach, particularly the mass analysis to understand the particles flows at the tire/road interface; and the dry lubrication theories developed for powders (as molybdenum disulfide MoS2 ) to understand and model the friction. Experiments are conducted in laboratory to understand and model this phenomenon. Experimental protocol allows simulating the particles' build up process on the road surface. The specimen surface, representative of a road surface, includes a microtexture scale, representing the asperities of the aggregates, and a macrotexture scale, representing the space between the aggregates. Friction measurements are realized by means of the so-called Skid Resistance Tester Pendulum, widely used in the road field, which simulates the friction between a rubber pad sliding at 3 m/s on the specimen surface. On a surface initially covered with particles, successive friction runs are performed, without resupplying particles between two consecutive runs. Specimen's weight is recorded before and after each friction run. Results show that friction drops significantly, compared to a clean state, when the surface is covered by particles. Successive runs induce an increase of friction coefficient until reaching a stable value which is below that of a clean surface. Three particles' flows are calculated: particles ejected from the contact area between the friction slider and the test surface; particles trapped by the surface microtexture; particles stored by the surface macrotexture. Close relationship was found between the friction coefficient and the flow of particles trapped by the microtexture. A first attempt of modeling allows to calculate the friction coefficient from the fraction of surface covered by particles.*


**Keywords :** *Friction, road pavement surface, fine particles, lubrication, modeling*

# 1 Introduction

Road statistics has pointed out an increase of accidents when it rains after a long dry period [1]. It has also been noticed a decrease of tire friction when the number of dry days since the last precipitation increases [2][3]. Persson et al. [4] attributed the risk excess induced by dry weather to the presence of fine particles (atmospheric dust, wear debris, etc.). These authors said that particles are mixed with water and create a viscous film which lubricate the tire/road interface. Despite this explanation and evidences about the risk induced by fine particles, physical mechanisms are not well understood and further investigations are needed. In particular, it is not clear whether particles reduces already friction on a dry road surface and how particles' characteristics affect friction.

In this paper, experiments are first performed to assess friction evolution on surfaces exhibiting different textures. Analyses are then conducted, based on a third body approach, to better understand the particles' flows at the tire/road contact area. Lubrication mechanisms are proposed in the light of these analyses and SEM observations. A simple model is then proposed to calculate the friction coefficient of a contaminated surface.

# 2 Experimental program

## 2.1 Test samples

Test samples are composed of two aluminum rectangular slabs of 130mm × 80mm × 15mm (surface of 130mm × 80 mm ≈ 0.01m$^2$). The first sample is sandblasted (Fig. 1a), called "Sandblasted" in the rest of the article, and the second sample is sandblasted and grooved (Fig. 1b), called "Chocolate". Surface treatments aim at creating surface roughness similar to that of a road surface: sandblasting (using corundum particles of diameter greater than 2 mm in size) creates the microtexture (fine asperities provided by aggregates which generate friction by defodrming the tire rubber); grooving creates the macrotexture (space between aggregates). Grooves have a triangular shape with a width of 2 mm at its basis and a depth of 1 mm. It allows creating a grid with regular squares of 10 mm aside.

a) 

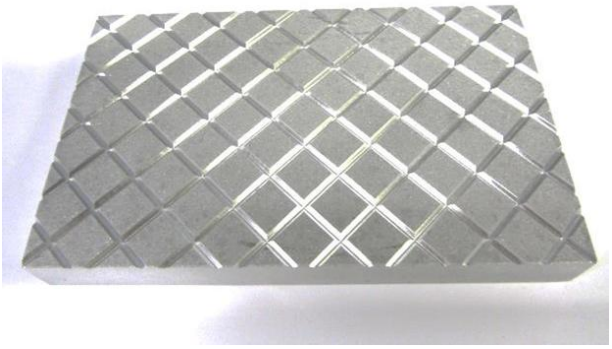

b)

Fig.1 Surfaces of (a) the sandblasted aluminum sample and (b) the grooved and sandblasted aluminum sample

## 2.2 Particles collecting and characterization

Particles are collected at the catchment area of Cheviré bridge, located near Nantes. This area collects runoff water coming from the South part of this bridge. This is due to the huge amount of particles needed for the experiments and the difficulties to collect them directly on the road surface. The daily traffic is 90,000 vehicles with 8.5% of trucks.

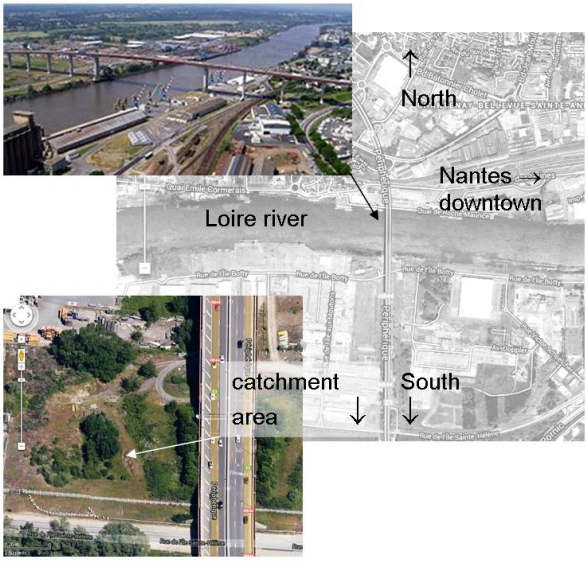


Fig.2 Cheviré bridge (near Nantes) and the catchment area

Particles are collected under the form of sediments, which are dried at 40°C during four days and sieved to keep only particles with a diameter inferior to 100 µm. This limit is based on literature review [5][6] which showed that only these small particles could have an effect on friction as they stick to the surface. SEM (Scanning Electron Microscopy) observation of the particles showed that they exhibit various shapes and sizes. Chemical analysis (Fig. 3) indicated that they are mainly composed of Silica and few other metallic elements that can be attributed to the wear of braking system and tires. The presence of Na, K and Mg can be

explained by industrial sites located next to the Cheviré bridge.

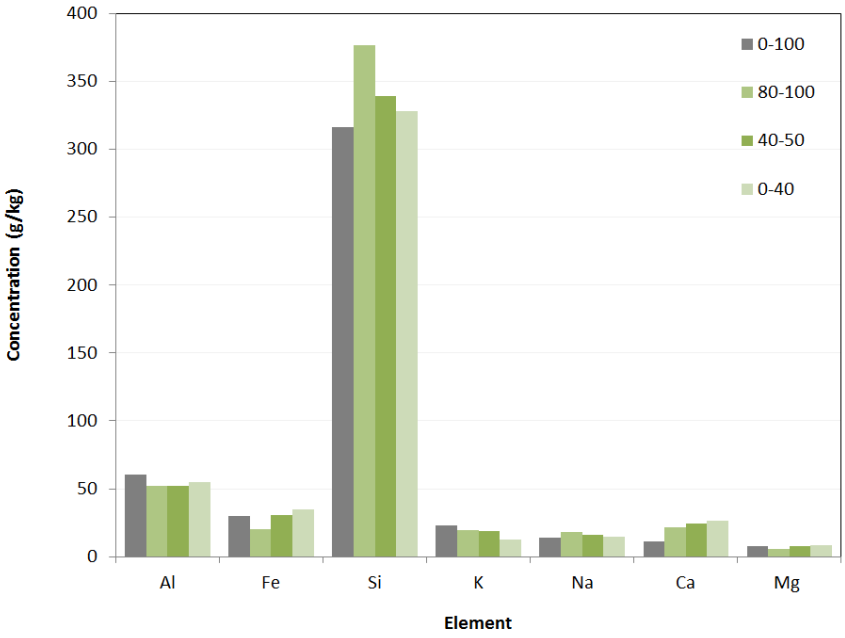


Fig.3 Chemical composition of the particles

## 2.3 Particles deposit and compaction

A quantity of 0.2g of dry particles is laid on the surface, which represents 20 g/m². This quantity is in the range of values for urban areas as reported in [7][8]. Thus, the surface covered by this amount of particles is rather similar visually to road surfaces after a long dry period.

a) 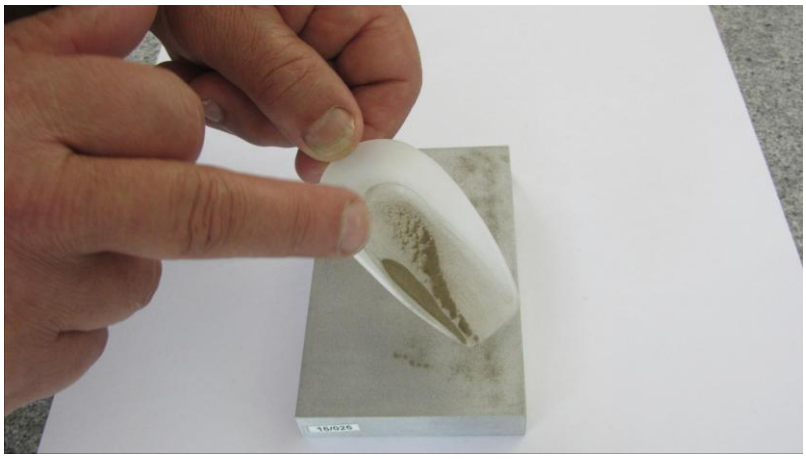

b)

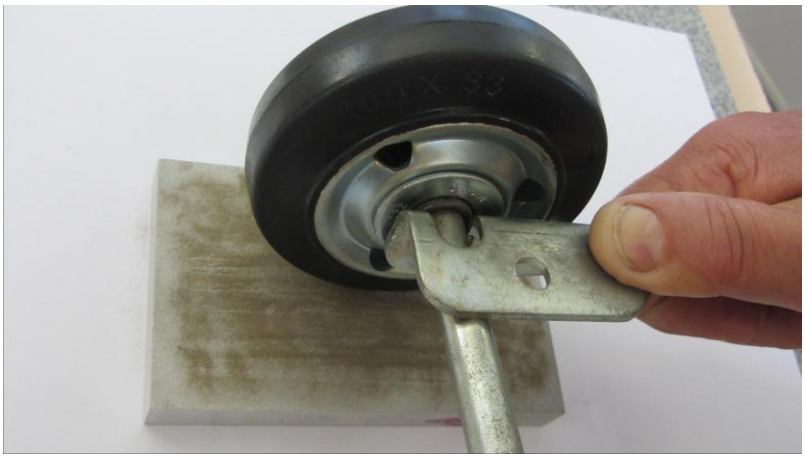

c)

Fig.4 Simulation of particle deposit (a: spreading; b: compaction; c: surface covered by particles)

Spreading of particles on the test surface is done manually (Fig. 4a). The particles are then compacted manually (simulation of vehicular traffic) by means of a small wheel mounted on a metallic arm (Fig. 4b). Specimens are subjected to repeated passes (60 passes) of the wheel. Care is taken to apply as much as possible the same wheel pressure to obtain a homogenous distribution of the particles. The repeatability of this method has been checked and was considered as satisfying.

## 2.4 Friction measurement

Friction is measured are realized with a Skid Resistance Tester Pendulum. This device can be used both in laboratory and on real road. It is composed of an articulated arm wearing a rubber pad, which slides on a wet test surface. The arm is initially in horizontal position. The arm is released and depending on the roughness of the tested surface, it moves up to a maximum height, whose value match to a "friction coefficient". The test procedure and the rubber characteristics are specified by European standards [9].

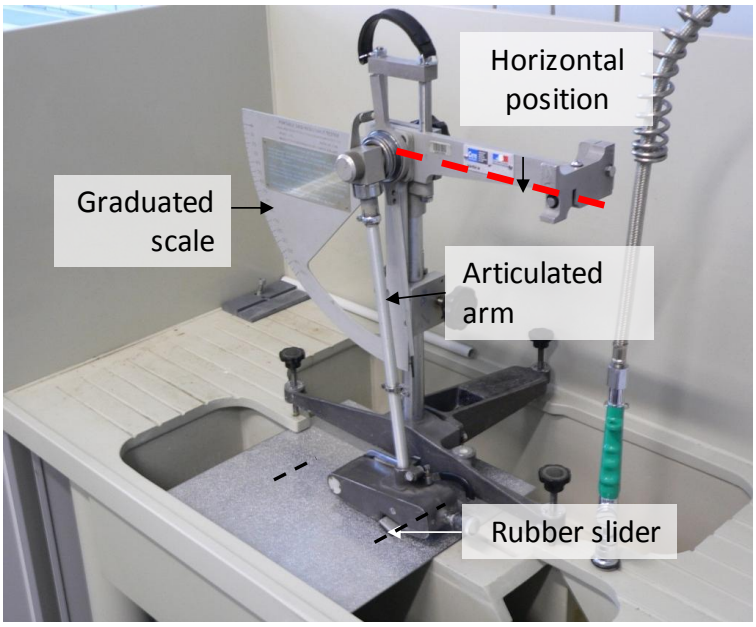


Fig.5 Skid Resistance Tester Pendulum

## 2.5 Test procedure

A test series comprises several steps as described below:

- On the dry and clean surface (step numbered 0): measurement of 3D height cartographies; weighing of the sample (mass $m_0$); friction measurement.
- Particles are deposited and compacted.
- On the contaminated surfaces (step numbered i, i ≥ 1): weighing of the sample (mass $m_{sample,i}^{before}$); friction measurement on dry-contaminated surface; weighing of the sample after friction measurement (mass $m_{sample,i}^{after}$).
- Steps (i) are repeated until values of the friction coefficient of three successive steps do not differ more than ± 0.01. End of the test series.

The criteria chosen to stop friction tests is directly linked to the reproducibility of the measurement method. A new rubber pad is used for each test series and the rubber is wiped after each friction measurement to limit the contamination of the surface.

In the meantime, the sample is weighed before and after each friction measurement in view of estimating the mass of particles before and after each run. These values can be then used in the third body approach developed in section 3.2.

Lastly 3D cartographies and SEM observation are performed on small areas of the samples.

# 3 Results

## 3.1 Friction analysis

Evolutions of friction coefficient for the two studied surfaces are presented in figure 6. The effect of the contaminants can be clearly seen because the friction coefficient of contaminated surfaces (steps i; $i \geq 1$) is always lower than that of a clean surface (step 0). For the two surfaces, friction coefficient is lowest at the beginning (step 1) then increases progressively with increasing number of slider passes until reaching a stable value.

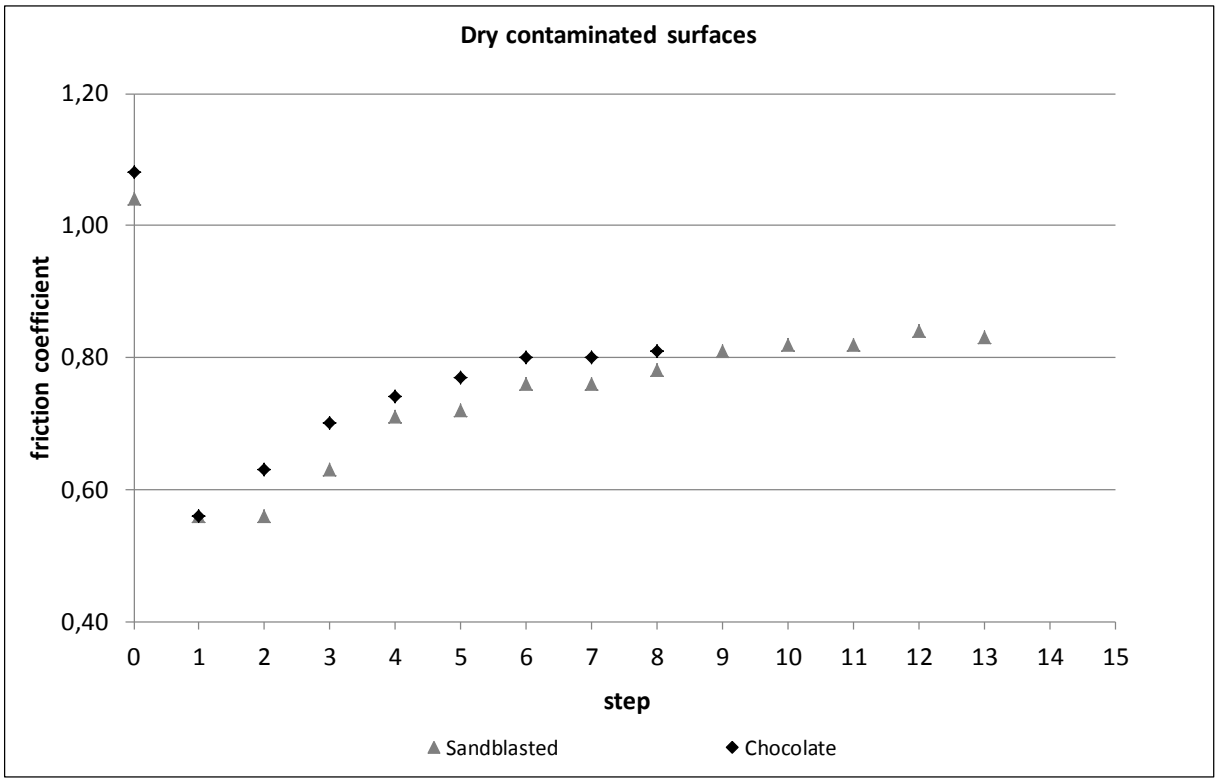


Fig.6 Variation of friction coefficient on contaminated surfaces

Even if the value at which the friction coefficient stabilizes is almost the same for the two surfaces (0.82 and 0.80 in average for respectively the Sandblasted and the Chocolate), the evolution towards friction stabilization is more rapid for the Chocolate (end of test series at step 8 instead of step 13 for the Sandblasted).

The initial and residual quantities of particles seem both to govern the friction variation. There is then a need to go further in the analysis to understand what happens at the friction slider/test sample interface. As the quantities of particles seem to be a crucial factor, it was thought that the analysis of mass of particles can be a relevant approach. Fillot et al. [10] have shown that the analysis of the wear-induced particles' mass and its link with particles' flows can help to better understand the movement of particles inside the contact and better interpret wear laws. Given the similarities between Fillot and coauthors' study and our study (movement of dry particles trapped between two rubbing surfaces), we think that the same

approach can be adopted for our study to better interpret friction variations.

## 3.2 Mass analysis

### 3.2.1 Calculation of particle mass from weighing

Weighing of the rubber slider shows that its mass loss during a test series is negligible (few milligrams) compared with the mass of introduced particles (hundreds of milligrams). Weighing of the sample at the beginning/end of each test series – clean state – shows that its weight does not change. The quantity of detached particles from the two contacting bodies (slider and sample) is then negligible and it was assumed in the following paragraphs that the weight difference between a contaminated sample and the dry-clean sample represents only the mass of the particles. Furthermore, it can be noticed that the mass of particles recorded after friction measurement at step (i-1) represents the mass of particles before friction measurement at step (i). Therefore, in the rest of the paper, for the sake of simplicity "mass of particles" refers to weighing before friction measurements.

From weighing (see test procedure), the mass of particles at a given step (i) can be extracted as follows:

$$m_{particles,i} = m_{specimen,i} - m_{specimen,0} \quad (1)$$

where $m_{particles,i}$ is the mass of particles at step (i); $m_{specimen,i}$ is the mass of the specimen at step (i); $m_{specimen,0}$ is the mass of the clean and dry specimen.

### 3.2.2 Relationship between friction and mass of particles before friction measurement

Figure 7 shows the friction variation with the mass of particles. It can be seen that the friction and particles' mass variations are identical but in the opposite directions: less particles induce more friction. Mills et al. [11] explained that there is a shear effect when the slider sweeps the particle layer and the initial layer of particles thins (and so the particles' mass decreases) to the point where the slider-surface asperity contact is restored. This mechanism can explain why friction starts from a minimum value (shearing mechanism), then increases with successive passes of the slider (sliding mechanism with partial contact between the rubber slider and the surface asperities).

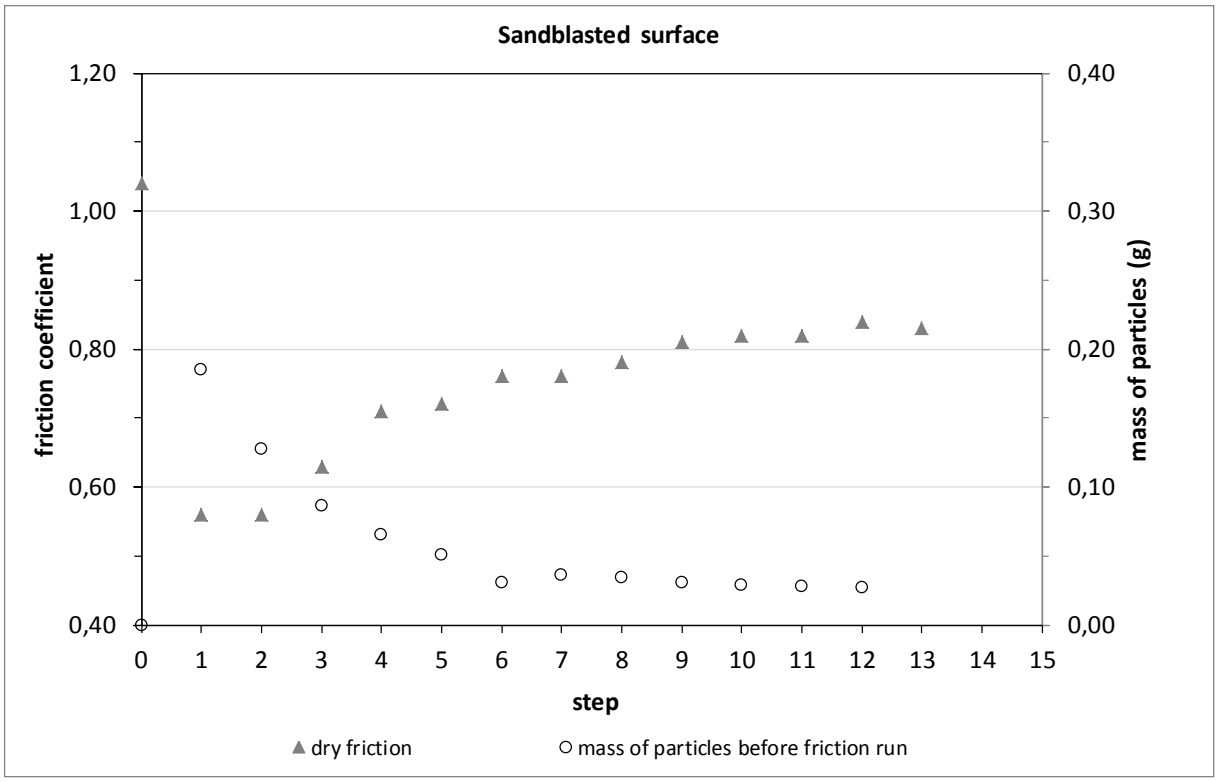


Fig.7 Variation of friction coefficient and particles mass (case of Sandblasted surface)

Figure 8 shows the relationship between friction and mass of particles for the two surfaces. In addition to the fact that less particles induce more friction, two other observations can be made. The first one is that there is a sharp increase of friction at the left end of the graph related to the Sandblasted (particles' mass lower than 0.05g). This observation was also made by Heshmat [12] for powder layers and this author attributes the sharp increase of friction to the breaking of the particle layer and then the beginning of direct contact between the two contacting bodies (considering powder as a third body).

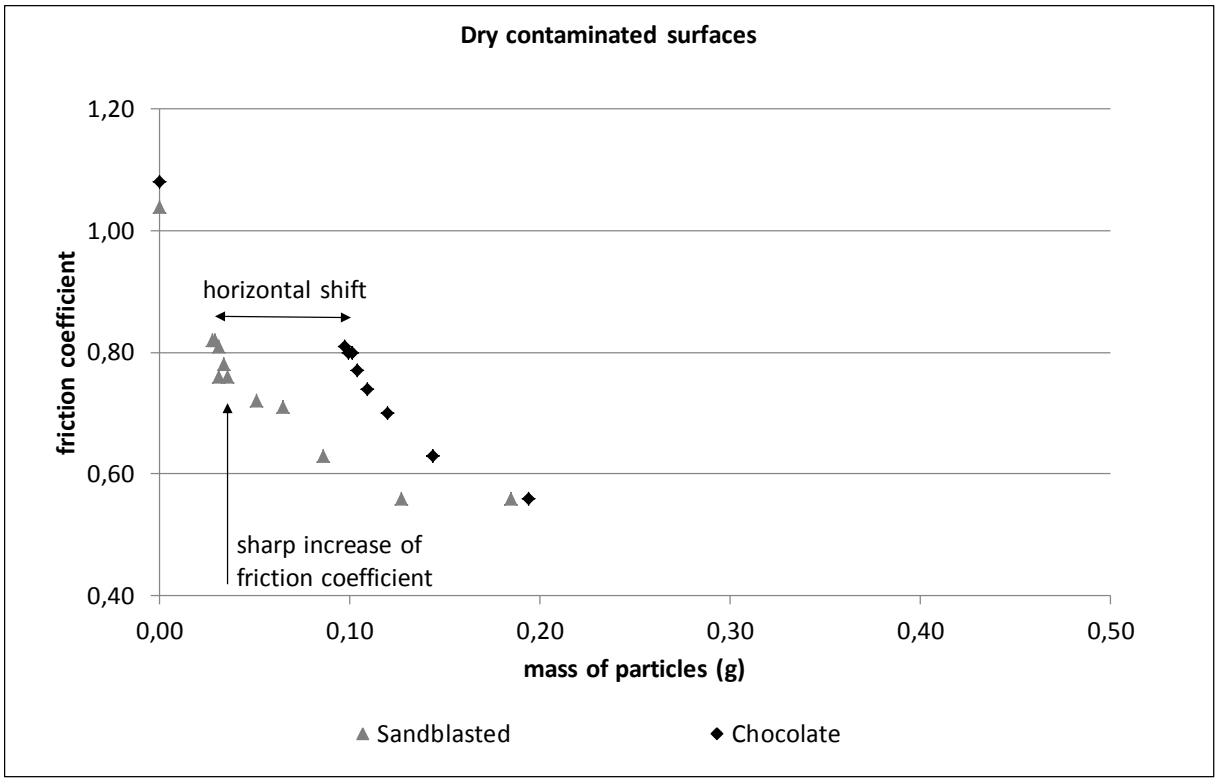


Fig.8 Variation of friction coefficient with particles mass

The second observation is that there is a horizontal shift between data related respectively to the Sandblasted and the Chocolate, meaning that the same friction coefficient does not correspond to the same particles' mass on the two surfaces. This surprising result can be attributed to the presence of grooves on the Chocolate. Actually, the weight of the Sandblasted specimen takes into account, after subtracting the weight of the clean specimen, particles present on the surface of the specimen whereas the weight of the Chocolate includes particles both on the surface and in the grooves. Therefore, to be comparable, weighing of the Chocolate must be corrected to remove the mass of particles stored in the grooves.

Figure 9a schematizes the Chocolate after compaction of the particles. It can be seen that part of the particles stays at the surface and part is stored in the grooves. When the friction slider passes over the surface, three particles' flows can be observed (Fig. 9b):

- Particles ejected from the surface by the slider;
- Particles pushed into the grooves by the slider;
- Particles retained, or trapped, by the surface microtexture.

On the three flows, only the second and the third ones are of interest because they affect directly the weighing result. A model is then proposed to separate these two flows in the weighing.

a)

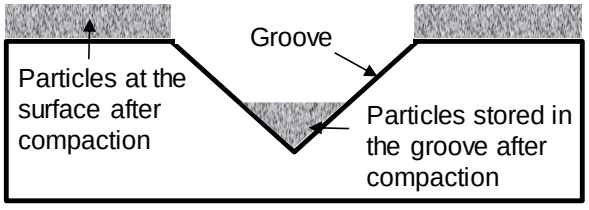

b)

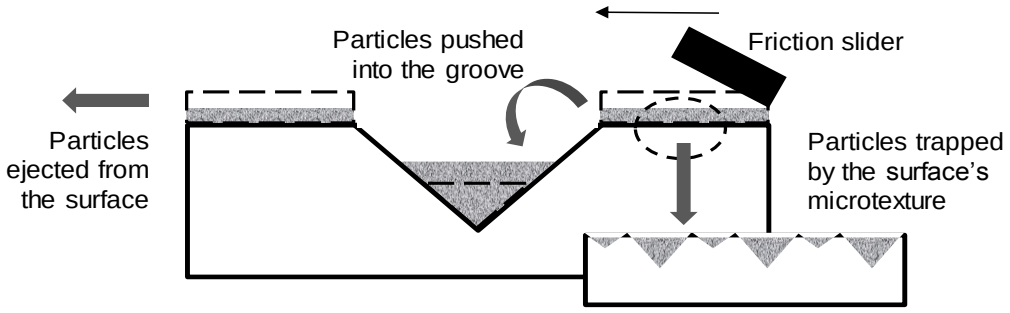


Fig.9 Schematic representation of particles' flows

In figure 10 right, the Chocolate specimen at step (i-1) is illustrated. The mass of particles at the surface is represented by $m_{i-1}$. At step i (Fig. 10 left), it is assumed that the additional – because there are already particles in the grooves at step (i-1) – quantity of particles pushed into the grooves is a fraction of $m_{i-1}$. The k number ($0 < k < 1$) represents this fraction which is supposed furthermore to be constant during a test series (for a given particles' concentration and size fraction).

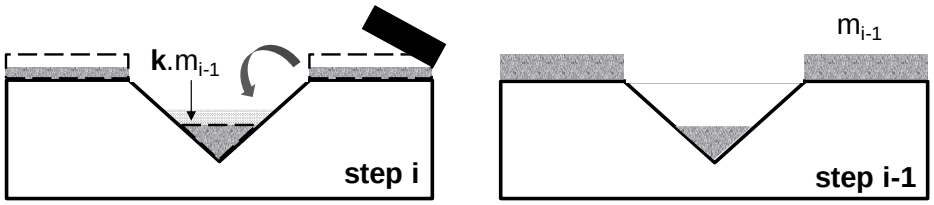


Fig.10 Assumed quantity of particles pushed into the grooves

The following equations can be then written:

$$m_{particles,i} = m^{surface}_{particles,i} + m^{groove}_{particles,i} \quad (2)$$

$$m^{groove}_{particles,i} = m^{groove}_{particles,i-1} + k\, m^{surface}_{particles,i-1} \quad (3)$$

Where $m_{particles,i}$ is the mass of particles at step (i); $m^{surface}_{particles,i}$ is the mass of particles at the surface of the specimen at step (i); $m^{groove}_{particles,i}$ is the mass of particles in the grooves at step (i); and k is the fraction of particles pushed into the grooves by the friction slider.

The above equations are valid for steps i ($i \geq 2$). For step 1, let us suppose that the quantity of particles in the grooves is a fraction (also represented by k) of the total quantity of particles (0.2g in the case of this study), meaning that:

$$m^{groove}_{particles,1} = k\, m_{particles,1} \quad (4)$$

It is therefore possible to estimate the quantity of particles in the grooves $m^{groove}_{particles,1}$ at

step 1 (Eq. 4) and at the surface $m^{surface}_{particles,1}$ ($m^{total}_{particles} - m^{groove}_{particles,1}$). These quantities are then used to estimate the quantity of particles in the grooves at step 2 $m^{groove}_{particles,1}$ (Eq. 3), from which the quantity of particles at the surface at step 2 $m^{surface}_{particles,1}$ can be deduced (Eq. 2). The calculations used at step 2 can be repeated for the following steps.

Factor k is obtained by assuming that, once the particles' mass at the surface of the Chocolate is determined, both surfaces Sandblasted and Chocolate should follow the same relationship relating friction to particles' mass. Physically, this assumption makes sense because the main difference between the Sandblasted and the Chocolate is the presence of grooves on the second and, once the effect of the grooves is removed, both surfaces should behave similarly with respect to friction. It means that k must be adjusted to superpose the two sets of data in figure 8.

Adjustments have been done using the Solver function of Excel and results are shown in figure 11.

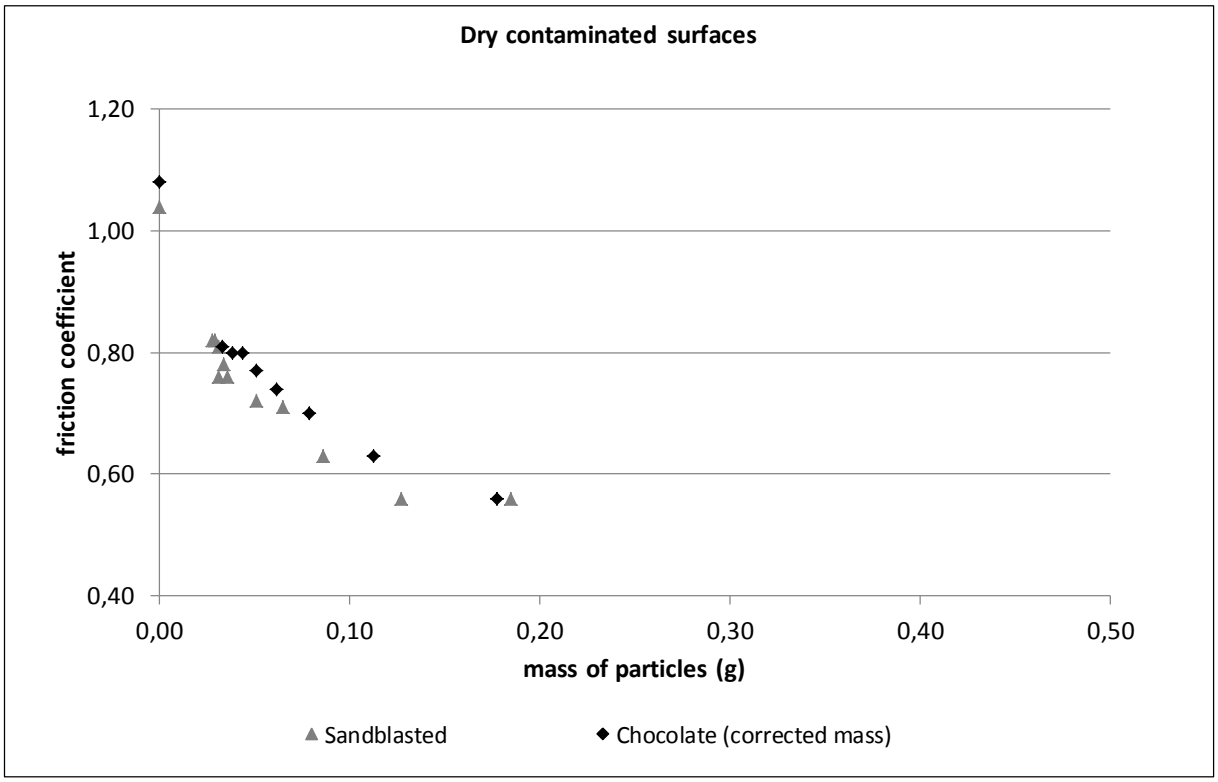


Fig.11 Variation of friction coefficient with the mass of particles at the surface of the specimens

The adjusted value of k is 0.085 and it can be seen that the superposition of Sandblasted's data on Chocolate's corrected data is satisfactory. The value of k means that at each pass, 8.5% of the mass of particles at the surface is pushed into the grooves. Looking at the dimensions of the Chocolate's tablets and grooves (Fig. 12), one can calculate the ratio between the grooves area (44 $mm^2$) and the tablet area (100 $mm^2$), which is 0.44. It means that if particles are pushed from the surface into the grooves, the maximum quantity should

represent 44% of what is present at the surface. While this calculation is crude and further analyses are needed, it shows that the adjusted value of k does not seem to be illogic.

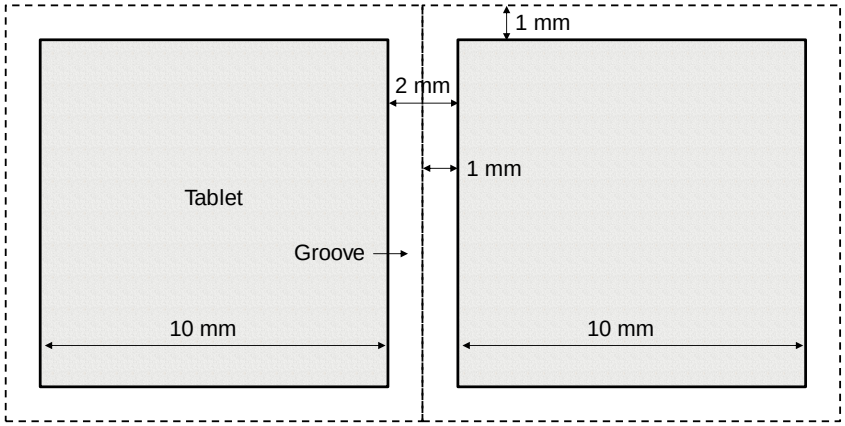


Fig.12 Dimensions of the tablets and the grooves

### 3.2.3 Covering of the surface and particle trapping

Figure 11 has pointed out the role of particles present at the surface with respect to friction. Visual observations are then conducted to better understand how particles affect friction. SEM pictures of the test surface were taken at two steps: surface after compaction of the particle layer (step 1); and surface after 5 friction runs. It can be seen that, after compaction, particles recover almost completely the sample surface (Fig. 13a) and, after some passes of the friction slider, only particles trapped in the surface valleys remain (Fig. 13b).

a) 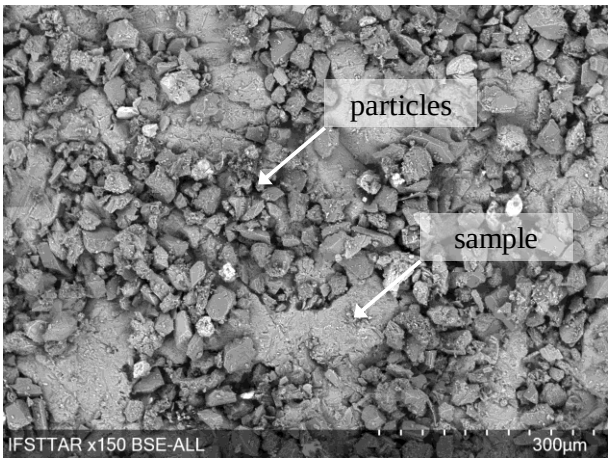

b) 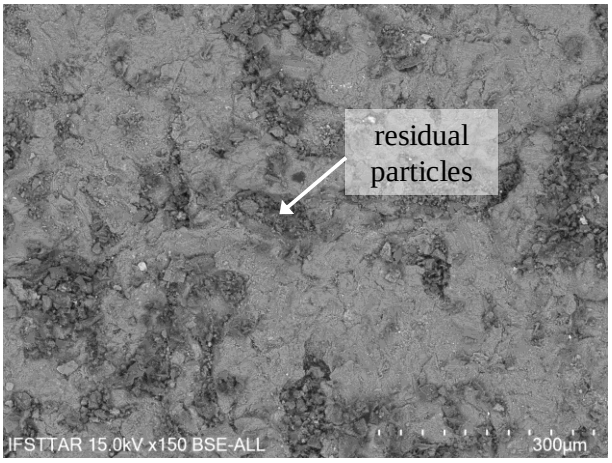


Fig.13 SEM visualizations of the surface of the sample (a: surface recovered by particles; b: surface after 5 friction runs)

Mills et al. [11] mentioned that when the sample surface is rough, it can induce some particles trapping (illustrated in Figure 9). The presence of trapped particles can explain why the friction coefficient at the end of a test series is lower than that of a clean surface. Attempt has been made to estimate the quantity of trapped particles from the surface texture considering two volume parameters: sum of $V_{vv}$ + $V_{vc}$ and $V_{vv}$. The first parameter considers all the valleys of a surface and the second only the deepest valleys. From table 2, the available volumes are:

- 175 $mm^3$ (sum $V_{vv}$ + $V_{vc}$ multiplied by the total surface = 17.52 × 0.01, then converted from ml to $mm^3$) and 18.2 $mm^3$ ($V_{vv}$ × total surface) for the Sandblasted. Assuming that fine particles are similar to clay (density of 1700 $kg/m^3$ or 1.7 $10^{-3}$ $g/mm^3$), the mass of particles that can be stored is respectively 0.297g (considering $V_{vv}$ + $V_{vc}$) and 0.031g (considering $V_{vv}$). These values will be called respectively "valley threshold" and "deep valley threshold".
- 123 $mm^3$ (sum $V_{vv}$ + $V_{vc}$) and 12.7 $mm^3$ ($V_{vv}$) giving respectively 0.208g and 0.022g of thresholds for the Chocolate.

The four mass thresholds are added to the graph in figure 11 and provide another insight into the relationship between friction and particles' mass (Fig. 14). When the mass of particles is lower than the valley threshold, friction coefficient starts to increase from a level which corresponds to $\mu_{lub}$ (dotted horizontal line at $\mu$ = 0.56). One can say that the valley threshold represents the theoretical minimum quantity of particles to cover completely all surface asperities. When particles are ejected and the mass of particles is lower than this threshold, some direct contacts are established between the slider and the surface asperities; the friction coefficient becomes then higher than $\mu_{lub}$.

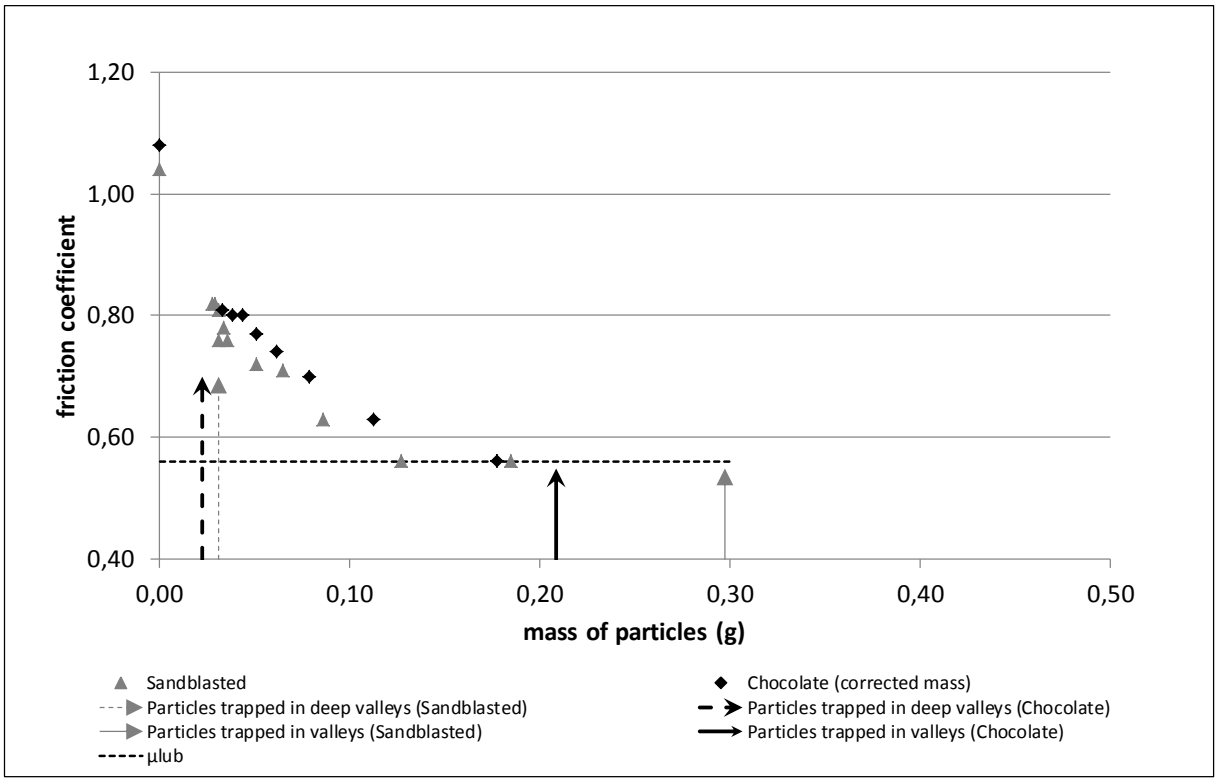


Fig.14 Variation of friction coefficient with the mass of particles and the role of trapped particles

Successive runs will eject other particles from the slider/specimen contact area. For the Sandblasted, table 1 shows that the deep valley threshold corresponds to the mass of particles at which the friction coefficient stabilizes. Unfortunately, it is not possible to draw the same conclusion with respect to the Chocolate for which the deep valley threshold is much lower than the mass of particles at which the friction coefficient stabilizes. Further tests and analyses are needed to clarify the role of particles trapped in the deepest valleys of the surface.

Tab.1 Values of friction coefficient and mass of particles

| Sandblasted | | Chocolate | |
|---|---|---|---|
| Mass of particles (g) | Friction coefficient | Mass of particles (g) (corrected) | Friction coefficient |
| 0,000 | 1,04 | 0,000 | 1,080 |
| 0,185 | 0,56 | 0,178 | 0,560 |
| 0,127 | 0,56 | 0,113 | 0,630 |
| 0,086 | 0,63 | 0,079 | 0,700 |
| 0,065 | 0,71 | 0,061 | 0,740 |
| 0,051 | 0,72 | 0,051 | 0,770 |
| 0,031 | 0,76 | **0,044** | 0,800 |
| 0,036 | 0,76 | 0,038 | 0,800 |
| 0,034 | 0,78 | 0,033 | 0,810 |
| **0,031** | 0,81 | | |

| | | | |
|---|---|---|---|
| 0,029<br>0,028 | 0,82<br>0,82 | | |

# 4 Modeling

## 4.1 Model formulation

From figure 6, it can be said that friction of surfaces contaminated by dry particles is between two extreme values: $\mu_{dry}$ (clean surface) and $\mu_{lub}$ (surface fully covered). It was seen that the mass of particles, or more exactly, the way by which the test surface is covered by particles, governs the friction coefficient. The friction coefficient of a contaminated surface can be then expressed as:

$$\mu = X\,\mu_{lub} + (1 - X)\mu_{dry} \tag{5}$$

where X is the fraction of the surface covered by the particles.

It can be seen that when X = 1 (surface fully covered), $\mu = \mu_{lub}$; when X = 0 (clean surface), $\mu = \mu_{dry}$. The term $\mu_{dry}$ expresses the unlubricated friction between the rubber and the test surface and includes preponderant mechanisms like hysteresis (dissipated energy) and adhesion (molecular bonds) [13]. The term $\mu_{lub}$ can include some rubber's deformation losses and mechanisms specific to particulate layers like shearing or rolling as Mills and coauthors highlighted in [11]. Modeling these two terms is a very complex task and is beyond the objective of this study. That is why $\mu_{dry}$ and $\mu_{lub}$ will be obtained by experiments.

Equation (5) is widely used in the literature and there are different ways to express X. In his theory of powder lubrication, Heshmat [12] noticed that "… the change in the friction coefficient value is due to the onset and growth of powder depletion with the duration of testing …". This author used a so-called index of starvation which expresses the evolution of the powder film from a full-film state to a partially-broken state and defined it as the ratio of available powder to the powder for full film. In the present study, using the mass of particles, an index of starvation $I_{starv}$ is calculated as the available quantity of particles at each step, i.e., $m_{particles,i}$, divided by the initial quantity of particles after compaction, i.e., $m_{particles,1}$:

$$I_{starv} = \frac{m_{particles,i}}{m_{particles,1}} \tag{6}$$

The index of starvation $I_{starv}$ has the same meaning as the fractional coverage X because the mass of particles $m_{particles,i}$ corresponds somewhat to the local height of third body film h; and $m_{particles,1}$ is the maximum of $m_{particles,i}$. We can check that for $I_{starv} = 0$ (no particle) $\mu = \mu_{dry}$ and for $I_{starv} = 1$ (surface fully covered) $\mu = \mu_{lub}$.

First attempts using equation (5) with $X = I_{starv}$ have shown that the model does not always fit the experiments. It was found that adding an exponent (n) to $I_{starv}$ gives better results. The

final form of the model tested in the present study is:

$$\mu = I_{starv}^{n}\,\mu_{lub} + (1 - I_{starv}^{n})\mu_{dry} \quad (7)$$

where n is an exponent to be determined.

## 4.2 Results

Figure 15 shows the comparison between the model and the experiments. It can be seen that the proposed model reproduces very well experimental results, in particular the increase of friction coefficient from the minimum and its stabilization. The lines representing the model is not smooth because the particles' mass (and so the index of starvation) does not evolve smoothly between successive steps. The relative error between the model and experimental values is less than 2% for all particles' sizes and concentration; it confirms the accuracy of the model.

Adjusted values of exponent (n) are 0.33 and 0.45 for respectively Sandblasted and Chocolate surfaces. For the moment, one possible interpretation of the physical meaning of exponent (n) could be connected to polydispersed particles' interaction [14]. Indeed, the size of tested particles ranges from 0 to 100 µm. Thus, the initial film of particles could act as a granular material, with numerous particles to particles interactions. As the size of particles is rather variable (analysis demonstrated a distribution centered around 50 µm and following a normal law), one can assume that particles exhibit a high cohesion. When the rubber pad passes over the contaminated surface, particles are moved and the fall down into the grooves of the Chocolate and do not anymore participate to the friction phenomenon. The rubber pad removes progressively layers of particles. In the case of Sandblasted surface, particles are rolled over the surface and their removal is slowier. Further investigations are in progress to improve the physical interpretation of (n).

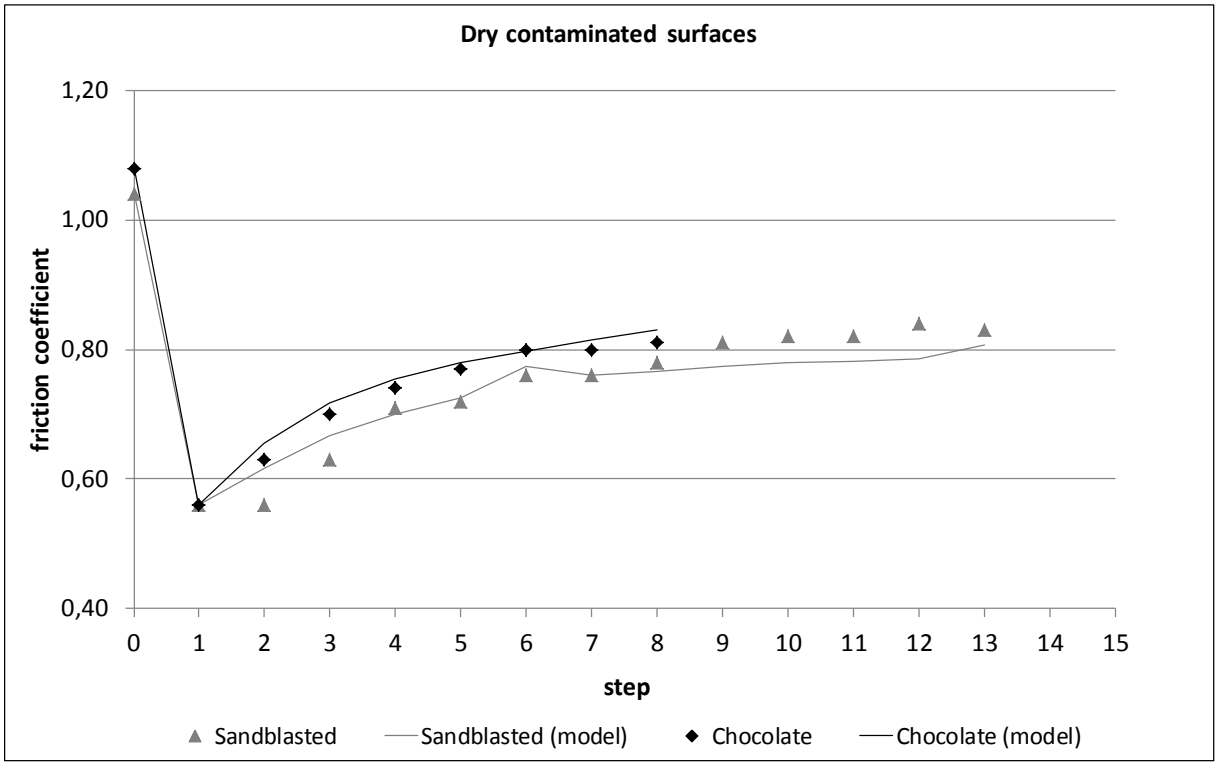


Fig.15 Model versus experimental results

# 5 Conclusions

This paper proposes a laboratory study of friction on dry road contaminated by fine particles deposited on the road surface. These particles are collected from a catchment area and sieved to keep only sizes lower than 100 µm. The test protocol simulates the particles' deposit, their compaction and they removal by the traffic. Sliding friction tests are conducted to evaluate the evolution of friction coefficient over time. Moreover, the study focused on the effect of two scales of surface texture: microtexture and macrotexture. Microtexture was obtained by sandblasting an aluminum sample whereas macrotexture was obtained by grooving the sample.

First of all, friction coefficient measured on contaminated surfaces is lower than friction on a clean surface expressed as $\mu_{dry}$ for both surface textures. The minimum value of friction coefficient, expressed as $\mu_{lub}$, was obtained at the first step of the experimental protocol when the surface is fully covered by a particles' layer. The successive runs induced an increase of the friction coefficient to a stable value which can be close to $\mu_{dry}$ or well below it.

Analyses of particles' mass at the various steps of the protocol showed that there was a tight relationship between friction and particles' mass: less particles induce higher friction. Explanations are given in terms of thinning of the particle layer by successive passes of the friction slider until asperity contact occurs. Estimation of the quantity of particles trapped by the surface texture helps to better understand the friction-particles' mass relationship. Two

mass thresholds were identified from the volume parameters (Abbott's curve). They determine respectively the moment when the friction coefficient increases from $\mu_{lub}$ and when it increases sharply to reach $\mu_{dry}$. In the meantime, a correction method for the particles' mass was developed for grooved surface. It was based on the assessment of the quantity of particles ejected in the grooves during each run. Thus, it was possible to estimate the amount of particles remaining in the contact area, which contributes to the friction generation.

In the last part, a simplified model was proposed to represent the friction coefficient of a contaminated surface as a function of $\mu_{lub}$ and $\mu_{dry}$ weighted by a function characterizing the surface fraction X covered by particles. It was found that X is best represented by the so-called index of starvation $I_{starv}$ developed for powder lubrication. Rising $I_{starv}$ to an exponent (n) provides very good adjustment of the model to the experiments. Further investigations are needed to clearly define the physical meaning of (n).

# 6 Acknowledgment

The authors thank Patrick Maisonneuve, Christophe Ropert and Jean-François Le Fur for the realization of all experiments.

# 7 References

[1] D. Eisenberg, The mixed effects of precipitation on traffic crashes. Accident Analysis and Prevention, 36, 637–647, 2004.

[2] R.B. Shakely, J.J. Henry, R.J. Heinsohn, Effects of pavement contaminants on skid resistance. Transportation Research Record, 788, 23-28, 1980.

[3] D. J. Wilson, An analysis of the seasonal and short-term variation of road pavement skid resistance. PhD Thesis, University of Auckland, NZ, 2006.

[4] B. N. J. Persson, U. Tartaglino, O. Albohr, and E. Tosatti, Rubber friction on wet and dry road surfaces: the sealing effect. Physical Review, B71, DOI: 10.1103/PhysRevB.71.035428, 2005.

[5] S. Descartes, C. Desrayaud and Y. Berthier, Experimental identification and characterization of the effects of contaminants in the wheel-rail contact. Proc. IMechE Part F: J. Rail and Rapid Transit, 222, 207-216, 2008.

[6] O. Arias-Cuevas, Z. Li, R. Lewis and E.A. Gallardo-Hernandez, Rolling-sliding laboratory tests of friction modifiers in dry and wet wheel-rail contacts. Wear, 268, 543-551, 2010.

[7] J. Vaze and F.H.S. Chiew, Experimental study of pollutant accumulation on an urban road surface. Urban Water, 4, 379-389, 2002.

[8] A. Deletic, D.W. Orr, Pollution build-up on road surfaces. J. Environmental Engineering, 131(1), 49-59, 2005.

[9] EN 13036-4: 2009, Method for measurement of slip/skid resistance of surface – Part 4: the Pendulum test, 2009.

[10] N. Fillot, I. Iordanoff, Y. Berthier, Wear modeling and the third body concept. Wear, 262, 949-957, 2007.

[11] R. Mills, R.S. Dwyer-Joyce, M. Loo-Morrey, The mechanisms of pedestrian slip on flooring contaminated with solid particles. Tribology International, 42, 403-412, 2009.

[12] H. Heshmat, Wear reduction systems for coal-fueled diesel engines – Experimental results and hydrodynamic model of powder lubrication. Wear, 162-164, 518-528, 1993.

[13] K.A. Grosch, The relation between the friction and visco-elastic properties of rubber, Proceedings of the Royal Society of London, Series A, Mathematical and Physical Sciences, 274(1356), 21-39, 1963.

[14] C. Voivret, Texture et comportement des matériaux granulaires à grande polydispersité, Thèse de doctorat, Université de Montpellier 2, 156 pages, 2008.